Observation of Ultracold Ground-State Heteronuclear Molecules

M. W. Mancini, G. D. Telles, A. R. L. Caires, V. S. Bagnato, and L. G. Marcassa

Instituto de Física de São Carlos, Universidade de São Paulo, Caixa Postal 369, 13560-970, São Carlos-SP Brazil

(Received 13 August 2003; published 2 April 2004)

We report the observation of translationally ultracold heteronuclear ground-state molecules in a two-species magneto-optical trap containing ^{39}K and ^{85}Rb atoms. The KRb molecules are produced via photoassociation and detected by multiphoton ionization. We had characterized their temperature and measured their formation rate constant. We believe that the two-species trap could be used as a reliable source of ultracold molecules to be captured by electrostatic, magnetic, or optical traps. This possibility will certainly motivate further investigation of quantum collective effects as well as high-resolution spectroscopy of the rovibrational level structure of cold heteronuclear molecular systems.

DOI: 10.1103/PhysRevLett.92.133203 PACS numbers: 34.50.Rk, 34.10.+x, 32.80.Pj

Ultracold molecules stands in a strategic position at the intersection of several powerful themes of research in atomic and molecular physics [1]. Recently, ultracold homonuclear alkali metal dimers formed in magneto-optical traps (MOTs) [2–5] have emerged as reliable sources of ultracold molecules. More recently, alternative decelerating schemes based on mechanical effects associated with the electric or magnetic dipole moments were proposed, extending the ability to trap and manipulate molecules [6–9] at very low temperatures.

The understanding of the molecular formation channels within a sample of cold and trapped atoms allows for the precise determination of the scattering length, whose values are important for evaluating the stability of the Bose-Einstein condensates (BECs) of alkali metal atoms [10]. They allow for controlling the formation of homonuclear ultracold ground-state molecules as well as its capture into optical and magnetic traps [5–9]. Ultracold molecules should prove to be useful in spectroscopy and the study of molecular structure, especially in ultrahigh resolution spectroscopy, which requires cold and trapped samples. Another especially promising area will be the study of collisions between ultracold molecules, in a regime where they behave like waves, perhaps giving rise to a new chemistry [11]. They may also allow for the study of collective quantum effects in molecular systems, including BEC [12]. Just as the laser cooling and trapping of neutral atoms a few years ago [1], the cooling and manipulation of cold molecules is likely opening up new branches of research. Finally, there are proposed experiments to study polar molecular systems in order to measure the electron's permanent electric dipole moment (EDM), the lifetime of long-lived energy levels, the effects of the dipole-dipole interactions on the molecular samples properties, etc. [13].

The investigation of samples containing two different atomic species in the cold regime has already reached the broad interest [14–16]. The KRb system has been explored in trap loss collision experiments [15,16] and also in elastic scattering yielding interspecies scattering lengths by measurements of the collisional rate between ^{41}K–^{87}Rb and ^{40}K–^{87}Rb [17]. Recently, the sympathetic cooling of these mixtures has lead to the achievement simultaneous quantum degeneracy of bosonic and fermionic species, producing BEC and Fermi-Bose mixtures [17,18]. Because of its mass and strong long-range dispersion coefficients, C_6, compared to the other heteronuclear alkali metal diatomic systems [19,20], KRb has very favorable Franck-Condon factors for the photoassociation spectroscopy [19,20].

In this work, translationally ultracold ground-state KRb molecules were produced by photoassociation, caused only by the rubidium trap laser beams, in a two-species MOT containing ^{85}Rb and ^{39}K atoms. The molecule formation starts with a pair of free ground-state atoms. After the quasiresonant absorption of a rubidium trap laser photon, the pair is promoted to a few rovibrational levels of one or more potentials correlating with an asymptote of one excited-state and one ground-state atom. In the next step, a small fraction of the photoexcited heteronuclear molecules spontaneously decay to bound levels of the ground-state singlet or triplet potentials correlating to a two free ground-state atoms, remaining translationally cold. The K*–Rb potentials, accessed by the K MOT trap laser beams, shall not play a role here because they present only repulsive long-range asymptotes.

Our MOT operates in a stainless chamber vapor cell with a background pressure below 10^{-8} torr. Two Ti:sapphire laser systems (Coherent 899-21) provide the laser beams for trapping Rb (780 nm) and K (766 nm). Electro-optical modulators (EOM) generate the repumping frequencies needed for the regular MOT operation. A single pair of coils, set up in anti-Helmholtz configuration, is used to generate the magnetic field gradients for trapping both samples. In typical experimental conditions the K and Rb samples are both loaded with an average of 10^7 atoms, presenting Gaussian spatial distributions with waists leading to maximum peak densities of about 2×10^9 cm^{-3} for K, and 3×10^{10} cm^{-3} for Rb. The overlap

between the samples is verified by monitoring the relative position of the atomic clouds by two CCD cameras. The number of trapped atoms is measured by calibrated photomultiplier tubes (PMTs). Further details about specific aspects of our experimental setup can be found elsewhere [15].

The KRb, K_2, and Rb_2 dimers formed into our MOT are detected by mass spectrometry using a channel electron multiplier (channeltron), after being photoionized. A pulsed dye laser (Continuum, Jaguar) pumped by the second harmonic of a Nd-doped yttrium aluminum garnet (Nd:YAG) laser (Continuum, Surelite I: 5 ns, 20 Hz repetition rate, 1.2 mJ/pulse), operating around 602.6 nm, provide the molecular ionization. This wavelength is near resonant with two-photon transitions connecting the ground-state atoms to the Rb (16D) and K (8D) atomic states. It was experimentally determined by scanning the pulsed dye laser between 600 and 610 nm, and it was optimized to produce the highest KRb^+ (time-of-flight) peak possible. This spectral region corresponds to the rubidium diffuse band, and it was studied earlier in light induced fluorescence experiments [21,22] and, more recently, it was used to detect ultracold Rb_2 dimers [3].

The experiment runs as follows: an external pulse delay generator (SRS, DG 535) provides the master clock and controls the switch on/off of all the lasers. The first step is to turn off the EOMs, which means switch off all the repumping frequencies. Then, another pulse with a controllable delay follows to the Nd:YAG laser triggering the ionizing laser shot. A fast photodiode detects the ionizing laser pulse for deriving the needed trigger for the time of flight (TOF). Furthermore, it is important to note that the ionizing laser illuminates the overlapped atomic clouds only after the MOT switch off with the shortest delay of about 200 μs, assuring that all the atoms and produced molecules are in their ground states. We have tried several different MOT switch off cycles, from two to 10 ms, to improve the TOF signal-to-noise ratio. The time sequence representing the experiment is shown in Fig. 1(a).

In Fig. 1(b) we present a typical TOF spectrum where the peaks due to K_2^+, KRb^+, and Rb_2^+ are very clear. The ratio between the TOF peaks due to KRb^+ (t_{KRb}), Rb_2^+ (t_{Rb_2}), and K_2^+ (t_{K_2}) are in agreement with those based on the mass ratios (e.g., $t_{\mathrm{KRb}}/t_{\mathrm{Rb}_2} \propto \sqrt{m_{\mathrm{KRb}}/m_{\mathrm{Rb}_2}} \simeq 0.854$). We have also checked that the peak due to KRb molecules fully depends on the existence of both K and Rb cold atomic samples. If one of the traps is not loaded, the KRb^+ peak does not appear in the TOF spectrum, assuring that the heteronuclear molecules are produced only by cold atoms inside the MOT. It is important to mention that the long time shoulder appearing in the Rb_2^+ ($\sim$ from 22 to 25 μs) is due to the Rb MOT spatial shape, which means that the Rb atomic cloud was elongated in the direction of the ionizing laser pathway. We checked that the signal due to the hot molecular ions formed in the

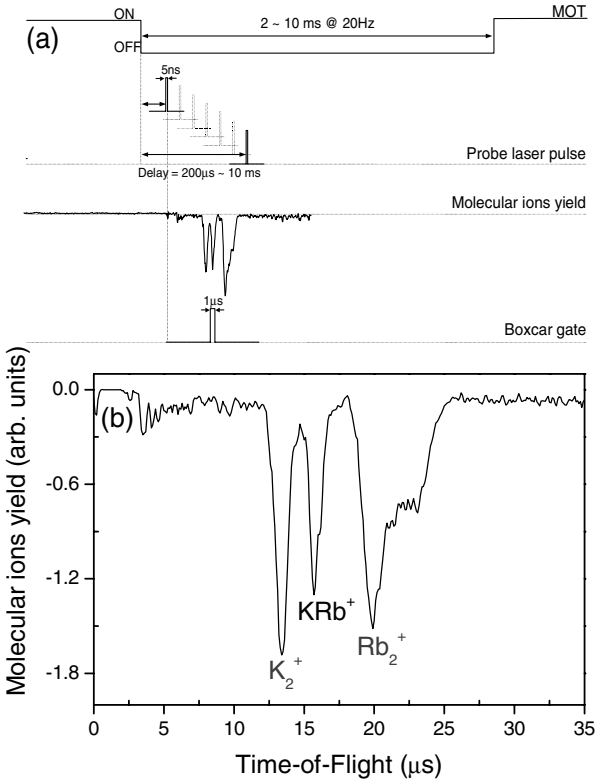

FIG. 1. (a) Experiment time sequence (not in scale) used to produce and detect the KRb molecules. (b) Time-of-flight spectrum showing the formation of heteronuclear molecules. The ratio between the TOF peaks due to KRb^+, Rb_2^+, and K_2^+ observed agrees with those based on the mass ratios (time shifts of $\pm 6\%$).

background vapor, as well as the atomic ions (hot and cold), is on the order of the measurement noise. We observed that the KRb^+ ion signal, shown in Fig. 1(b), strongly depends on the good overlap between the two atomic clouds and the ionizing laser beam. The translational temperature of the K_2, KRb, and Rb_2 molecules were measured by detecting the molecular ions as a function of the delay between the ionizing laser pulse and the trapping lasers switching off. A simple Monte Carlo numerical simulation allowed us to fit the time evolution of the molecular signal to determine the molecules' temperature. We found average temperatures of about 150 μK for KRb, 90 μK for Rb_2, and 250 μK for K_2 respectively, in good agreement with earlier published results [3–5]. The molecular temperatures found here are in agreement with the cold atomic samples from where they are produced, e.g., $T(\mathrm{Rb}) \simeq 180$ μK. We checked that the MOT coils do not play a role for the measured temperatures.

In Fig. 2 we present a diagram illustrating the proposed formation and detection mechanisms for the produced ground-state heteronuclear KRb ultracold molecules. The best potential energy curves found in the literature [23,24] for the molecular KRb were used in Fig. 2. To a good approximation, the whole process can be

represented by the following equations:

$$\mathrm{K}(4S_{1/2}) + \mathrm{Rb}(5S_{1/2}) + \hbar\omega_{\mathrm{Rb}} \rightarrow \mathrm{K}(4S_{1/2}) + \mathrm{Rb}(5P_{3/2}) \rightarrow \mathrm{KRb}^*(\Omega), \quad \mathrm{KRb}^*(^{1,3}\Lambda) - \hbar\omega_{\mathrm{spont}} \rightarrow \mathrm{KRb}(^{1,3}\Sigma^+), \quad (1)$$

$$\mathrm{KRb}(^{1,3}\Sigma^+) + 2\hbar\omega_p \rightarrow \mathrm{KRb}^+ + e^-. \quad (2)$$

The molecule formation starts with a pair of ground/excited atoms, attracted one to each other by dispersive long-range, van der Waals, forces represented by a $-C_6R^{-6}$ interaction, undergoing quasiresonant absorption of a rubidium trap laser photon, ω_{Rb}; $\mathrm{KRb}^*(\Omega)$ represents the excited molecular Hund's case (c) potentials with bound levels populated at long-range by the Rb trap laser photons in the step 1 (Fig. 2), and $\mathrm{KRb}^*(^{1,3}\Lambda)$ are the short-range excited molecular Hund's case (a) potentials ($^{1,3}\Pi$) connected to $\mathrm{KRb}^*(\Omega)$ potentials [25]. In the next step, a fraction of the photoexcited heteronuclear molecules spontaneously decays to bound levels of the ground-state molecular potentials KRb ($X^1\Sigma^+$ and $a^3\Sigma^+$) after emitting a photon with frequency ω_{spont}, step 2 (Fig. 2). Furthermore, the spontaneous decay rate may be enhanced by resonant coupling between two different potential curves of same symmetry, as suggested for the homonuclear case [26]. The detection process is a two-photon transition promoting the ground-state KRb molecules to a distribution of bound levels of the KRb^+ ground-state potential (steps three and 4, Fig. 2), asymptotically correlated to the $\mathrm{K}(4S) + \mathrm{Rb}^+ + e^-$ dissociation limit. It is represented by Eq. (2), where ω_p is the frequency of the ionizing pulsed dye laser. The produced KRb^+ molecules are stable until reaching the channeltron. If they dissociate [$\mathrm{KRb}^+ \rightarrow \mathrm{K}(4S) + \mathrm{Rb}^+$] before reaching the detector, the TOF spectrum will be different than that shown in Fig. 1(b).

The KRb triplet ground state, $a^3\Sigma^+$, presents a very shallow well with a longer range minimum compared to the singlet state, $X^1\Sigma^+$, indicating that its bound levels may be populated, contributing to the molecular signal observed. Note that the two atoms of different species interact via shorter range van der Waals forces when compared to the homonuclear dipole-dipole interaction, $-C_3/R^3$. Thus, in general, the wave function overlap between the initial free-atom ground state and the excited molecular bound state is significantly smaller than in a homonuclear system for a given excited-state binding energy. An important consequence of this short-range character of the excited molecular states is larger Franck-Condon decay factors to deeper bound vibrational levels of the singlet ground state, $X^1\Sigma^+$. It is important to mention that we are not able to distinguish between the molecules formed in ground singlet and/or triplet states. Finally, the potential energy curves of the electronic molecular states dissociating at the asymptotic limit $\mathrm{K}(4P_{3/2}) + \mathrm{Rb}(5S_{1/2})$ are all repulsive at long-range [19,20], hence they are not expected to contribute to the detected KRb molecular signal.

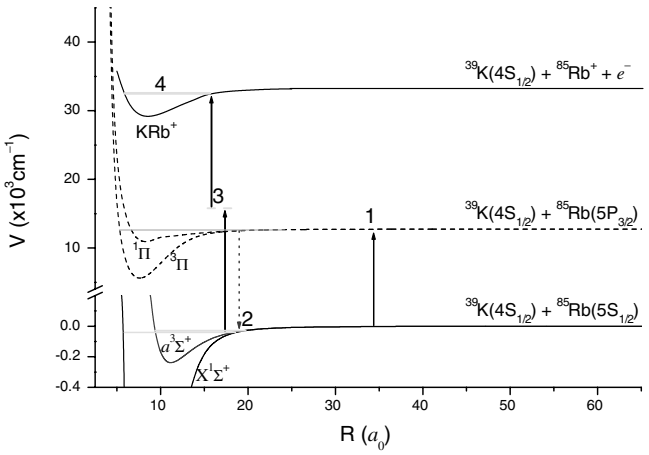

FIG. 2. Molecular formation channel proposed for the KRb ultracold molecules and the detection channel.

We have also checked the KRb^+ molecular ion signal dependence on the square of the dye laser energy, as shown in Fig. 3(a). It allows one to conclude that the ionization step proceeds via a two-photon transition from the molecular ground state, in agreement with the diagram shown in Fig. 2. In Fig. 3(b), we show the KRb^+ molecular ion signal as a function of Rb MOT density for two different densities of K trap. From the linear dependence observed in the plot, we concluded that the KRb^+ ion signal is proportional to the product of the MOT atomic densities as proposed below, also in agreement with the mechanism proposed in Fig. 2.

The KRb^+ molecule formation may be characterized by the following rate equation: $d[\mathrm{KRb}^+]/dt = K' n_{\mathrm{K}} n_{\mathrm{Rb}} \times V_{\mathrm{overlap}}$, where $d[\mathrm{KRb}^+]/dt$ represents the molecular ion signal rate, V_{overlap} is the intersection volume between the K and Rb MOTs, n_{K}, and n_{Rb} are the atomic densities of the K and Rb cold samples, respectively, and K' is the KRb^+ formation rate constant. We estimate the KRb formation rate constant to be on the order of 10^{-11} cm^3/s. To obtain this value we have assumed that, at the best experimental conditions, around 100 molecules/pulse are detected. This assumption is based on the characteristic time and amplitude response of our channeltron observed for a single molecular ion. Assuming a 50% total detection efficiency and that the ultracold molecules stay in the trap region for a characteristic time of about 2 ms [27] we find a molecular formation rate of about 10^5 molecules/s which leads to a formation rate constant, $K' \sim 8 \times 10^{-12}$ cm^3/s. Comparing this value to recent theoretical predictions [28], a very good agreement is obtained. We are building a new experimental setup in order to perform photoassociative spectroscopy of the KRb to determine and explore the rovibrational levels populated during the molecule formation.

In conclusion, we have observed the formation of heteronuclear ultracold ground-state molecules in a

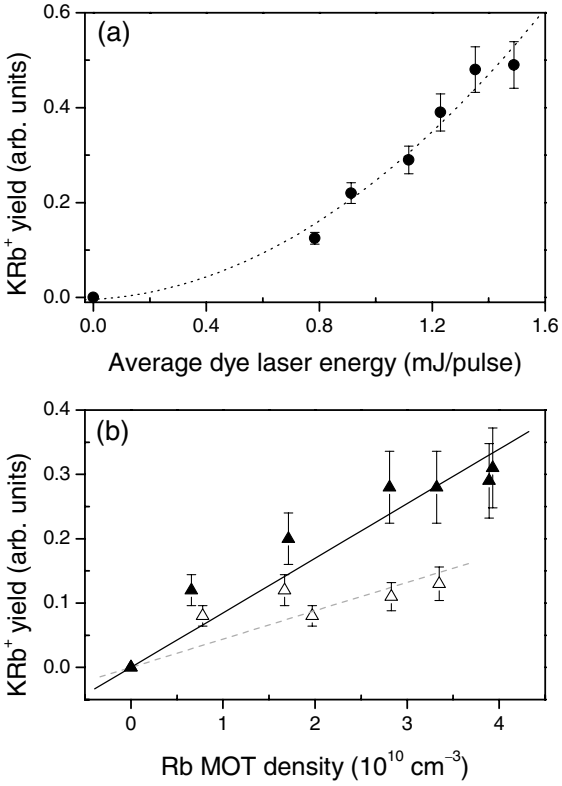

FIG. 3. (a) Ion signal as a function of the pulsed dye laser energy. The quadratic behavior with the pulsed laser energy (dotted line fit) assures the molecular ionization by two-photon transitions. (b) TOF peak value of the KRb^+ molecular ion yield as a function of the Rb MOT density, for two different K MOT densities: 1.7×10^{10} cm^{-3} (full up triangles), and 1.2×10^{10} cm^{-3} (hollow up triangles). The lines are fits assuming the linear dependence on the Rb MOT density, in good agreement with the experimental data.

two-species MOT using pulsed multiphoton ionization. We have characterized their temperature and proposed a reasonable molecule formation scheme based on the photoassociation of a pair of cold Rb and K atoms. This possible channel is in agreement with the observed density and the light intensity dependences of the molecular ion signal. The rate constant for the formation of the ultracold molecules was determined, and we hope this work will stimulate additional experimental and theoretical efforts in this way. Because of the relatively high molecule formation rate, we believe that the two-species MOT may provide a continuous source of ultracold molecules to be trapped and manipulated by electrostatic, magnetic, or optical traps. We also believe it will soon be useful in spectroscopic studies as well as in the production of molecular quantum gases [12].

We thank V. Nascimento for technical help. This work was supported by FAPESP (Fundação de Amparo à pesquisa do Estado de São Paulo).

[1] J. Weiner, V. S. Bagnato, S. C. Zilio, and P. Julienne, Rev. Mod. Phys. **71**, 1 (1999).
[2] A. Fioretti *et al.*, Phys. Rev. Lett. **80**, 4402 (1998); A. Fioretti *et al.*, Eur. Phys. J. D **5**, 389 (1999).
[3] C. Gabbanini *et al.*, Phys. Rev. Lett. **84**, 2814 (2000); A. Fioretti *et al.*, Eur. Phys. J. D **15**, 189 (2001).
[4] A. N. Nikolov *et al.*, Phys. Rev. Lett. **82**, 703 (1999); **84**, 246 (2000).
[5] T. Takekoshi, B. M. Patterson, and R. J. Knize, Phys. Rev. Lett. **81**, 5105 (1998).
[6] J. D. Weinstein *et al.*, Nature (London) **395**, 148 (1998).
[7] H. L. Bethlem, G. Berden, and G. Meijer, Phys. Rev. Lett. **83**, 1558 (1999).
[8] J. A. Maddi, T. P. Dinneen, and H. Gould, Phys. Rev. A **60**, 3882 (1999).
[9] N. Vanhaecke *et al.*, Phys. Rev. Lett. **89**, 063001 (2002).
[10] C. C. Bradley, C. A. Sackett, J. J. Tollett, and R. G. Hulet, Phys. Rev. Lett. **75**, 1687 (1995).
[11] D. J. Heinzen, R. Wynar, P. D. Drummond, and K. V. Kheruntsyan, Phys. Rev. Lett. **84**, 5029 (2000).
[12] J. Herbig *et al.*, Science **301**, 1510 (2003).
[13] H. Bethlem and G. Meijer, Int. Rev. Phys. Chem. **22**, 73 (2003).
[14] M. S. Santos *et al.*, Phys. Rev. A **52**, R4340 (1995); G. D. Telles *et al.*, Phys. Rev. A **59**, R23 (1999); U. Schlöder *et al.*, Eur. Phys. J. D **7**, 331 (1999); J. P. Shaffer, W. Chalupczak, and N. P. Bigelow, Phys. Rev. A **60**, R3365 (1999); Y. E. Young, R. Ejnisman, J. P. Shaffer, and N. P. Bigelow, Phys. Rev. A **62**, 055403 (2000); G. D. Telles *et al.*, Phys. Rev. A **63**, 0033406 (2001).
[15] L. G. Marcassa, G. D. Telles, S. R. Muniz, and V. S. Bagnato, Phys. Rev. A **63**, 013413 (2001); J. Goldwin, S. B. Papp, B. DeMarco, and D. S. Jin, Phys. Rev. A **65**, 021402(R) (2002).
[16] G. Ferrari *et al.*, Phys. Rev. Lett. **89**, 053202 (2002).
[17] G. Roati, F. Riboli, G. Modugno, and M. Inguscio, Phys. Rev. Lett. **89**, 150403 (2002).
[18] G. Modugno *et al.*, Science **294**, 1320 (2001); **297**, 2240 (2002).
[19] M. Marinescu and H. R. Sadeghpour, Phys. Rev. A **59**, 390 (1999).
[20] H. Wang and W. C. Stwalley, J. Chem. Phys. **108**, 5767 (1998).
[21] R. Beuc, S. Milosevic, and G. Pichler, J. Phys. B **17**, 739 (1984).
[22] G. Pichler, S. Milosevic, D. Veza, and R. Beuc, J. Phys. B **16**, 4619 (1983).
[23] S. Rousseau, A. R. Allouche, and M. Aubert-Frécon, J. Mol. Spectrosc. **203**, 235 (2000).
[24] A. Valance, J. Chem. Phys. **69**, 355 (1978).
[25] E. Tiemann, in *Interactions in Ultracold Gases from Atoms to Molecules*, edited by M. Weidemüller and C. Zimmermann (Wiley-VCH GmbH & Co. KGaA, Weinheim, 2003), p. 206.
[26] C. M. Dion *et al.*, Phys. Rev. Lett. **86**, 2253 (2001).
[27] D. Comparat *et al.*, Eur. Phys. J. D **11**, 59 (2000).
[28] O. Dulieu (private communication).